Science Advances

AAAS

advances.sciencemag.org/cgi/content/full/4/4/eaar2334/DC1

Supplementary Materials for

Evo-devo models of tooth development and the origin of hominoid molar diversity

Alejandra Ortiz, Shara E. Bailey, Gary T. Schwartz, Jean-Jacques Hublin, Matthew M. Skinner

Published 11 April 2018, *Sci. Adv.* **4**, eaar2334 (2018)
DOI: 10.1126/sciadv.aar2334

This PDF file includes:

Supplementary Materials and Methods

Micro-computed tomography and three-dimensional surface reconstruction

Scanning was conducted on a SKYSCAN 1172 Desktop Scanner using the following parameters: 100 kV, 94 µA, 2.0 mm aluminum and copper filter, 0.12 rotation step, 360 degrees of rotation, and 2-frame averaging. Raw projections were converted into TIFF image stacks using NRecon with the isometric voxel dimensions of the resultant images ranging from 14 to 30 micrometers. The complete image stack of each tooth was filtered using a computer-programmed macro that employs a three-dimensional median and mean-of-least-variance filter (each with a kernel size of three) to improve tissue gray-scale homogeneity (*34*) and then manually segmented into enamel and dentine components using Avizo/Amira (FEI Visualization Sciences Group). Only teeth with minor wear (equivalent to Molnar's [*35*] first three wear stages) and well-distinguished gray-scale pixel values were segmented and used in the study. After segmentation, enamel-dentine junction (EDJ) surfaces were each reconstructed as a triangle-based surface model (surface generation module using the *unconstrained smoothing* parameter). When necessary, small missing parts of the EDJ due to wear or damage were reconstructed in Geomagic Studio (3D Systems) following the curvature of teeth. Reconstruction of 18 damaged teeth were performed twice and differences between reconstructions were non-significant (paired-*t* test; *t*: 0.1951; *p*-value: 0.8476; df: 17). The digital models of the EDJ were manipulated on Avizo/Amira for landmark digitizing and trait scoring.

Scoring procedures

The expression of upper molar cusp 5 (UMC5) and lower molar cusps 5, 6, and 7 (LMC5, LMC6, and LMC7) was scored following the Arizona State University Dental Anthropology System (ASUDAS) (*36*), with minor modifications specified in table S4. Morphological manifestations of mesiolingual features (including Carabelli's cusp) of the upper molars differ markedly among hominoids (*25*, *37-41*). For simplicity, all mesiolingual features are referred to as Carabelli's cusp, although homology of these features among taxa remains unknown (*25*). Scoring criteria for Carabelli's cusp followed those of (*25*) and (*40*) for great apes and australopiths, respectively. Carabelli's cusp expression in later hominins was recorded using the ASUDAS (*36*). The expression of UM hypocone, upper molar cusp 6 (UMC6), and LM "double" C6 was scored as either present or absent.

To facilitate statistical analyses, Carabelli's cusp was subsequently classified into four categories: "absent", "faint", "medium", and "large" (table S4). Similarly, expression of UMC5, LMC5, LMC6 and LMC7 was divided into "absent" (ASUDAS grade 0), "suspected", "faint" (ASUDAS grade 1), "medium" (ASUDAS grades 2-3), and "large" (ASUDAS grades 4-5). As per (*18*) the "suspected" category indicates the presence of a subtle bump on the marginal ridge that may represent a poorly developed accessory cusp. All data were observed and collected at the EDJ. Skinner and Gunz (*18*) also suggested that poorly developed or "suspected" LMC6 could represent instances in which the available space between adjacent cusps allowed the formation of a new secondary enamel knot whose growth as a cusp did not progress substantially due to the onset of calcification of the tooth crown. This not only applies to "suspected" LMC6, but likely also to all other accessory cusps. In all instances in which accessory cusp data were only analyzed by presence/absence, teeth having the "suspected" category were not included.
In order to test for intra-observer error in scoring cusp expression, 25 randomly selected teeth were scored twice by AO, with scoring sessions separated by six weeks. Error was 2.67%, which

is similar or lower than that previously reported (*42-43*). Only two cases of trait disagreement between the two scoring sessions were found, with this disagreement being of one grade only. No disagreements in trait presence (vs. absence) were observed.

<u>Intercusp distance</u>
Three-dimensional landmarks were digitized on the EDJ using Avizo. In addition to serving as a proxy for the final shape of the inner enamel epithelium (IEE) of the developing tooth germ, using the EDJ allows the cusp apices (dentine horns) to be located with greater accuracy than at the outer enamel surface, especially when tooth wear is not extensive (*24*). This is important considering that measurement error in intercusp distances reported by (*17*, *19*) was up to 30% for their two-dimensional analyses of recent *H. sapiens* upper molars at the enamel surface.

First, second, and third molars were pooled and separated into groups according to the number of cusps (i.e., upper molars with four, five or six cusps and lower molars with four, five, six or seven cusps). This was done to maximize sample size per fossil taxon, and given that the PCM was formulated to explain cusp number and size regardless of tooth type, this approach should not alter the final outcome of the study. In each group, homologous landmarks were placed at the tip of the dentine horns of all cusps present such that the number of landmarks corresponds to the total number of cusps in the tooth crown. No grouping was exclusively based on Carabelli's cusp given that this feature is not necessarily associated with the presence of a dentine horn, which is only seen on ASUDAS grades 5-7 (*25*). For the four main cusps (protocone, paracone, metacone, and hypocone) of the upper molars, the first landmark was placed on the tip of the protocone and subsequent points were placed following a buccal direction on the tip of the paracone, metacone, and hypocone, respectively. When accessory cusps were present, landmarks on the tip of cusps 5 and 6 were placed after the landmark associated with the hypocone. Collection of landmarks on the lower molars started at the tip of the protoconid, with subsequent landmarks made on the cusp tips of the metaconid, entoconid, hypoconid, and when present, the hypoconulid, entoconulid, and metaconulid in that order (fig. S3). This order follows the general sequence of cusp development extensively documented for humans and other primates (*44-47*) Intercusp distances (Euclidean distances) were derived from these landmarks, and given that they were placed on 3D surface models, these Euclidean distances account for cusp differences in both height and position.

<u>Tooth size</u>
Tooth size at the EDJ was estimated in three different ways. First, tooth size was obtained from crown outlines as per (*17*, *19-20*). To that end, each 3D model was manually oriented so that the occlusal surface was perpendicular to the optical axis of the screen and the main buccolingual and mesiodistal grooves are parallel to the x- and y-axes, respectively. Once in proper orientation, a scale was added, and screenshots of the crown occlusal surface were saved as .jpg files. The area of the crown outline of each tooth was calculated in Adobe Photoshop®. We also followed Skinner and Gunz's (*18*) 3D geometric morphometrics approach and used centroid size as a proxy for tooth size. To calculate centroid size, a set of landmarks was digitized along the upper and lower molar marginal ridge, with the first landmark placed at the midpoint of the mesial marginal ridge between the two mesial cusps. Subsequent landmarks were digitized following a buccal and lingual direction for upper and lower molars, respectively. After the first coordinate, all subsequent landmarks were placed at the lowest point on the marginal ridge of

two given adjacent cusps. Neither "suspected" cusps nor cusp 7 were considered when collecting this second set of landmarks. The use of the mesial marginal ridge, however, may underestimate tooth size in taxa where the base of the crown is much wider than the occlusal surface. Finally, we calculated the 3D surface area of the EDJ crown (*32*) in Rhino 5.0 (Robert McNeel & Associates). To ensure consistency among specimens, we followed recommendations by (*33*) in which all 3D models were first simplified to 10,000 faces and smoothed at 100 iterations with a 0.6 lambda value using Avizo/Amira. Following previous studies (*17*, *19-20*), the square root of the 2D and 3D crown area was used for statistical analysis.

As shown in fig. S4 and table S5, there is a high and significant correlation among the three different estimates of tooth size. Given that tooth size was ultimately used as a proxy for the duration of crown morphogenesis and size of the IEE, developmentally, the reasonable approach was to use 3D surface area to test how well the PCM explains molar cuspal patterns.

<u>Statistical analysis</u>

All statistical analyses were performed in PAST (*48*) or R (*49*; packages "MASS" and "VGAM"). Unless otherwise noted, differences were considered significant at $\alpha = 0.05$. Following (*17*), the non-parametric Kendall's rank correlation test and ordered logistic regression (OLR) models were used to examine the relationship between relative intercusp spacing (i.e., intercusp distance divided by tooth size) and the presence and degree of expression of accessory cusps. While the former test evaluates only the strength and direction of this relationship, OLR assumes a causal relationship between variables such that accessory cusp expression (response variable) is modeled as a factor of relative intercusp distance (explanatory variable). Each OLR model yields a single coefficient value (from which the odds ratio is calculated) and separate intercepts for each cut-point between grades of expression (*50*). As per (*17*, *19*) a value of 0.1 equals a unit in relative intercusp distance, with odds ratios also scaled to this value. The overall fit of the models was evaluated with the likelihood ratio test (G) in comparison to the null or constant-only model in which a single value is associated with the explanatory variable. In all cases, calculation of the average intercusp distances was based on the spacing between all previously-formed cusps to the exclusion of the accessory cusp being studied. Analyses on single intercusp distances were also conducted to assess whether, for any given accessory cusp, the spacing of adjacent cusps more strongly influence its presence and expression.

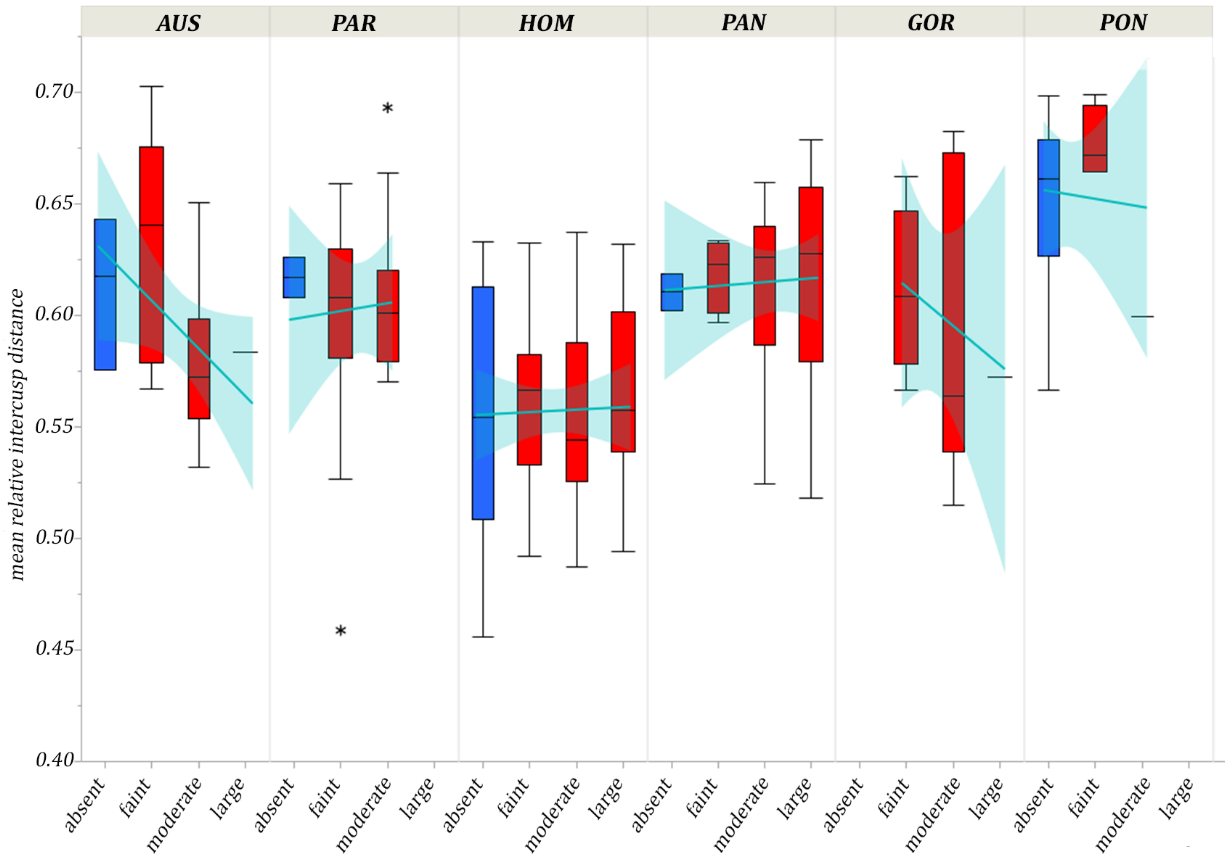

fig. S1. Relationship between mean relative intercusp distance and Carabelli's cusp per genus. Line of fit and 95% confidence intervals for each dataset added in light blue only for visualization purposes. The PCM predicts a negative relationship between Carabelli's cusp expression and mean relative intercusp distance. For box plots, cusp absence in blue and cusp presence (faint to large) in red. Abbreviations, AUS: *Australopithecus*, PAR: *Paranthropus*, HOM: *Homo*, PAN: *Pan*, GOR: *Gorilla*, and PON: *Pongo*.

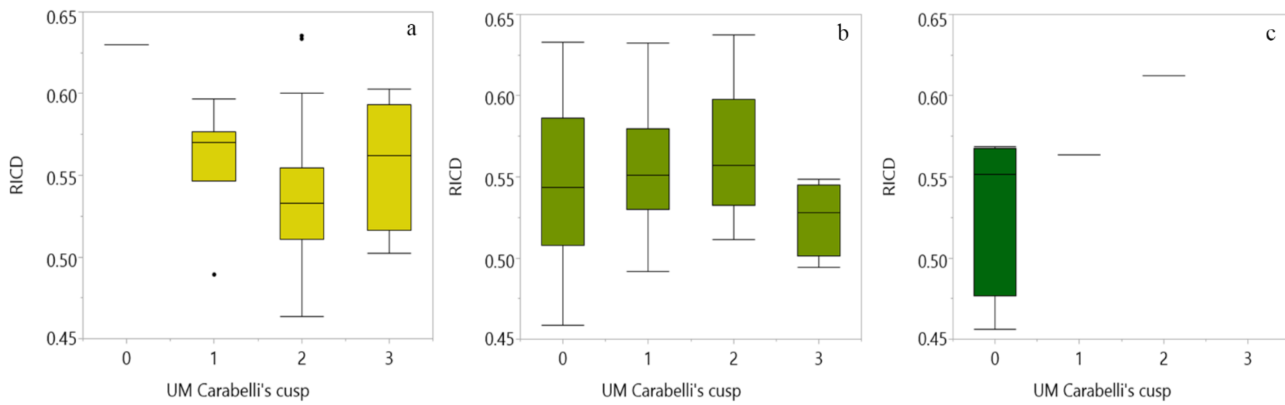

fig. S2. Relationship between mean relative intercusp distance and Carabelli's cusp per molar type in *Homo*. Scores: 0=absent; 1=faint CC present; 2=medium-sized CC present; 3=large CC present. The PCM predicts a negative relationship between Carabelli's cusp expression and RICD. Upper (a) M1, (b) M2, and (c) M3 analyzed independently to assess whether the timing of molar development influences the applicability of the PCM.

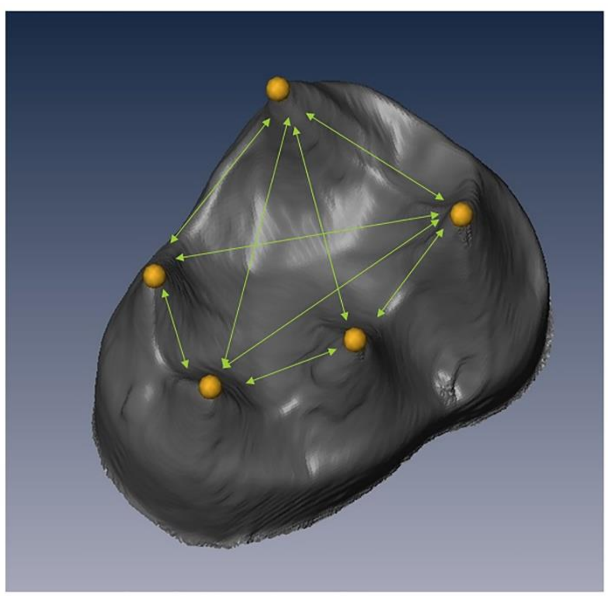

fig. S3. Right lower molar with example of homologous landmarks (yellow dots) placed at the cusp tips from which Euclidean distances were calculated. Arrows indicate pairwise distances taken for each tooth.

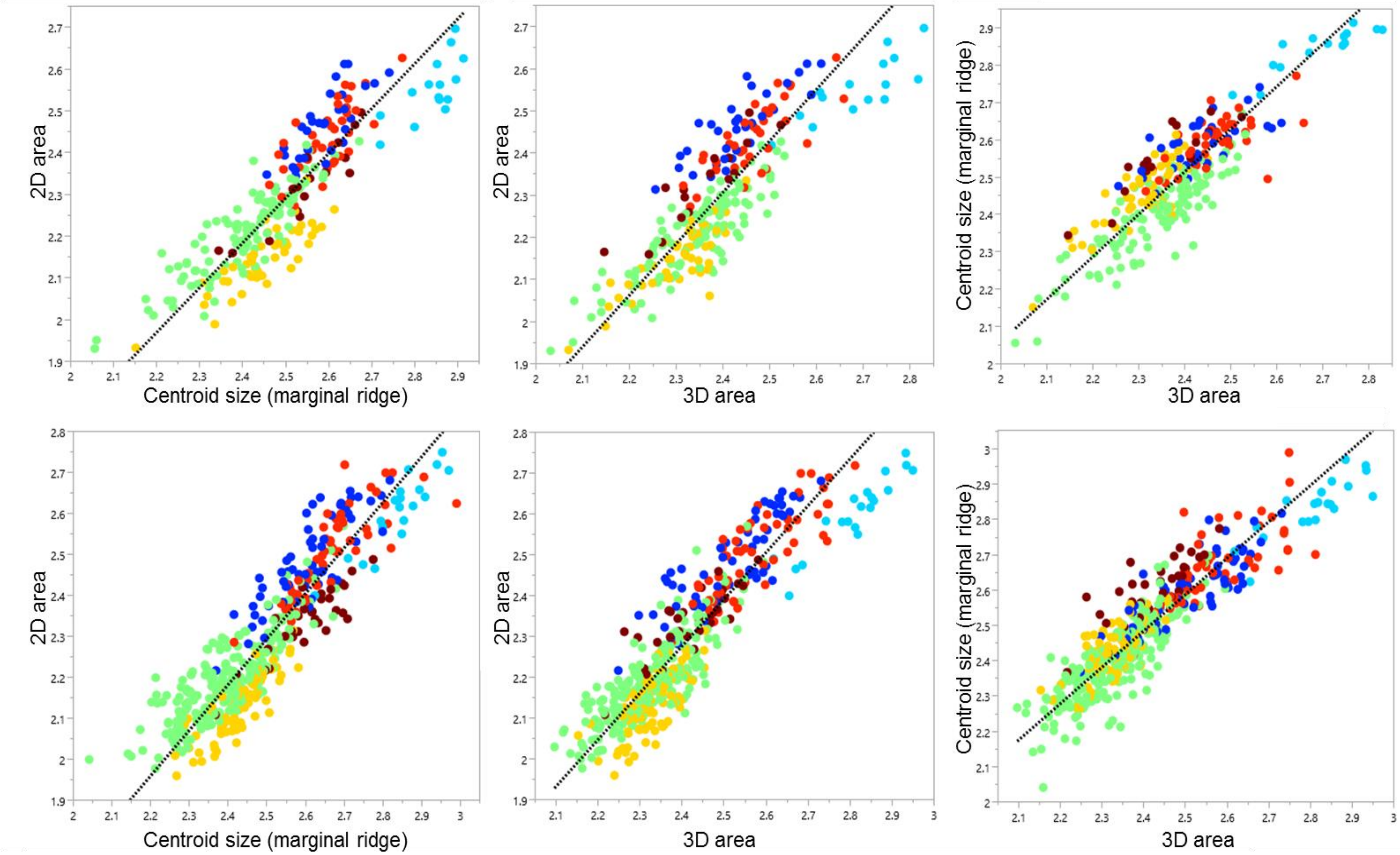

fig. S4. Ordinary least squares regression of upper (top row) and lower (bottom row) molar size comparisons estimated from crown outline, centroid size, and 3D surface area. Comparisons performed on the logged data. Legend: *Australopithecus*: blue; *Paranthropus*: red; *Homo*: light green; *Pan*: yellow; *Gorilla*: light blue; *Pongo*: brown.

table S1. Ordered logistic regression of cusp expression and relative intercusp distance.

Taxon	n	Cusp	Relative distance	Coefficient	Intercept 0|1	1|2	2|3	3|4	4|5	df	AIC	LL (h1)	LL (h0)	p-value*	odds**
Australopithecus	24		mean	-19.04	-13.57	-12.13	-7.91	N/A	N/A	72	52.53	-22.27	-24.31	**< 0.05**	0.15
Paranthropus	24		mean	2.79	-0.73	1.85	-	N/A	N/A	48	50.15	-22.08	-22.13	N.S.	1.32
Homo	79	Carabelli's cusp	mean	0.75	-1.21	0.03	2.35	N/A	N/A	237	206.51	-99.26	-99.27	N.S.	1.08
H. sapiens (recent)	35		mean	9.95	3.56	5.23	7.26	N/A	N/A	105	95.65	-43.82	-44.50	N.S.	2.70
Pan	35		mean	2.10	-1.52	-0.29	1.35	N/A	N/A	105	86.98	-39.49	-39.52	N.S.	1.23
Gorillla	11		mean	-7.50	-	-4.71	-2.14	N/A	N/A	22	26.10	-10.05	-10.28	N.S.	0.47
Australopithecus	35		me-hyp	9.87	6.66	7.51	7.76	8.84	9.57	175	83.36	-35.68	-36.82	N.S.	2.68
Paranthropus	39		me-hyp	13.79	8.36	9.67		11.64		117	81.94	-36.97	-38.78	N.S.	3.97
Homo	113	UM cusp 5	me-hyp	-0.36	0.65	1.85	2.26	3.41	4.53	565	226.77	-107.39	-107.39	N.S.	0.96
H. sapiens (recent)	49		me-hyp	5.89	4.22	5.74	6.05	-	-	147	86.96	-39.48	-39.94	N.S.	1.80
Pan	49		me-hyp	2.75	2.56	4.07	4.80	5.52	-	196	93.42	-41.71	-41.85	N.S.	1.32
Homo	144	LM cusp 5	end-hyd	39.39	19.41	19.46		20.11	N/A	432	202.30	-97.15	-138.39	**< 0.001**	51.37
H. sapiens (recent)	104		end-hyd	40.49		20.58		21.21	N/A	208	136.22	-65.11	-96.21	**< 0.001**	57.34
Australopithecus	48		end-hylid	25.66	11.46	12.02	13.04	-	N/A	144	13.04	-38.44	-47.70	< 0.001	13.01
Paranthropus	46		end-hylid	19.41	7.09	7.51	8.46	13.04	N/A	184	112.36	-51.18	-55.94	**< 0.01**	6.97
Homo	127	LM cusp 6	end-hylid	21.87	10.25	10.65	11.19	15.24	N/A	508	211.29	-100.65	-118.52	**< 0.001**	8.91
H. sapiens (recent)	67		end-hylid	28.62	14.26	14.68		17.90	N/A	201	77.88	-34.94	-44.97	**< 0.001**	17.50
Pan	69		end-hylid	18.31	6.99	7.81	8.54	12.53	N/A	276	189.86	-89.93	-95.75	**< 0.001**	6.24
Pongo	29		end-hylid	44.13	23.23		23.65	25.24	N/A	87	31.32	-11.66	-15.79	**< 0.01**	82.52
Australopithecus	19		med-end	19.11	10.25	11.40	11.85	13.86	N/A	76	50.06	-20.03	-22.64	**< 0.05**	6.76
Homo	39	LM cusp 7	med-end	8.81	5.31	6.57		-	N/A	78	65.49	-29.75	-30.41	N.S.	2.41
Pan	46		med-end	4.00	3.28	5.10	5.82	-	N/A	138	68.70	-30.35	-30.48	N.S.	1.49

Genera not included indicate that the feature was invariably absent/present or that samples did not possess enough grades of expression/number of specimens for statistical analysis

LL (h1): log-likelihood of estimated model; LL (h0): log-likelihood of null model; df: degrees of freedom; AIC: Akaike information criterion

me: metacone; hyp: hypocone; med: metaconid; end: entoconid; hyd: hypoconid; hylid: hypoconulid; N/A: not applicable

* *p* -value of likelihood ratio test (significant values bolded); N.S.: non-significant

** odds ratios scaled to 0.1 as per Hunter et al. (*17*)

table S2. Fossil hominin upper molars used in this study including accession number, locality/site, and source.

Taxon	Specimen ID	Locality/Site (Country)	UM1	UM2	UM3	UM12	UM
A. anamensis	KNM-ER 30200	Koobi Fora (Kenya)	X	X			
A. anamensis	KNM-ER 30745	Koobi Fora (Kenya)	X				
A. anamensis	KNM-ER 7727	Koobi Fora (Kenya)		X			
A. anamensis	KNM-KP 34725g	Kanapoi (Kenya)		X			
A. afarensis	AL 200-1a	Hadar (Ethiopia)		X			
A. afarensis	AL 333-86	Hadar (Ethiopia)	X				
A. cf. *afarensis*	KNM-WT 16003	West Turkana (Kenya)			X		
A. afarensis	L 144-23	Omo (Ethiopia)	X				
A. cf. *afarensis*	Omo 18-1970-17992	Omo (Ethiopia)				X	
A. africanus	MLD 28	Makapansgat (South Africa)			X		
A. africanus	STS 1	Sterkfontein (South Africa)	X				
A. africanus	STS 212	Sterkfontein (South Africa)				X	
A. africanus	STS 24a	Sterkfontein (South Africa)	X				
A. africanus	STS 28	Sterkfontein (South Africa)		X			
A. africanus	STS 30	Sterkfontein (South Africa)		X			
A. africanus	STS 37	Sterkfontein (South Africa)		X			
A. africanus	STS 52	Sterkfontein (South Africa)		X	X		
A. africanus	STS 56	Sterkfontein (South Africa)	X	X			
A. africanus	STS 8	Sterkfontein (South Africa)	X	X			
A. africanus	STS 22	Sterkfontein (South Africa)		X			
A. africanus	STW 179	Sterkfontein (South Africa)			X		
A. africanus	STW 183	Sterkfontein (South Africa)	X	X			
A. africanus	STW 189	Sterkfontein (South Africa)			X		
A. africanus	STW 252j	Sterkfontein (South Africa)	X				
A. africanus	STW 402	Sterkfontein (South Africa)	X				
A. africanus	STW 450	Sterkfontein (South Africa)	X				
A. africanus	STW 529	Sterkfontein (South Africa)		X			
A. africanus	STW 140	Sterkfontein (South Africa)			X		

A. africanus	STW 151	Sterkfontein (South Africa)	X		
A. africanus	STW 183 (STW 128)	Sterkfontein (South Africa)			X
A. africanus	STW 280	Sterkfontein (South Africa)		X	
A. africanus	Taung	Taung (South Africa)	X	X	
A. africanus	TM 1561	Sterkfontein (South Africa)			X
P. boisei	KNM-WT 17400	West Turkana (Kenya)	X	X	X
P. robustus	DNH 3	Drimolen (South Africa)			X
P. robustus	DNH 54	Drimolen (South Africa)			X
P. robustus	DNH 57b	Drimolen (South Africa)	X		
P. robustus	DNH 60a	Drimolen (South Africa)	X		
P. robustus	DNH 62	Drimolen (South Africa)	X		
P. robustus	DNH 74	Drimolen (South Africa)		X	
P. robustus	SK 13.14	Swartkrans (South Africa)	X	X	X
P. robustus	SK 14129a	Swartkrans (South Africa)	X		
P. robustus	SK 16.1591	Swartkrans (South Africa)	X	X	
P. robustus	SK 41	Swartkrans (South Africa)			X
P. robustus	SK 47	Swartkrans (South Africa)	X	X	
P. robustus	SK 48	Swartkrans (South Africa)	X	X	X
P. robustus	SK 49	Swartkrans (South Africa)		X	
P. robustus	SK 52	Swartkrans (South Africa)	X	X	
P. robustus	SK 826a2	Swartkrans (South Africa)		X	
P. robustus	SK 829	Swartkrans (South Africa)	X		
P. robustus	SK 831a	Swartkrans (South Africa)			X
P. robustus	SK 832	Swartkrans (South Africa)	X		
P. robustus	SK 834	Swartkrans (South Africa)		X	
P. robustus	SK 838a	Swartkrans (South Africa)	X		
P. robustus	SK 102	Swartkrans (South Africa)	X		
P. robustus	SK 89	Swartkrans (South Africa)	X		
P. robustus	SKW 33	Swartkrans (South Africa)		X	
P. robustus	SKX 21841	Swartkrans (South Africa)			X
P. robustus	TM 1517a	Kromdraai (South Africa)	X	X	

P. robustus	TM 1517c	Kromdraai (South Africa)		X	X		
P. robustus	TM 1601e	Kromdraai (South Africa)	X				
Homo sp./*habilis s.l.*	DNH 39	Drimolen (South Africa)	X				
Homo sp./*habilis s.l.*	DNH 70	Drimolen (South Africa)	X				
Homo sp./*habilis s.l.*	KNM-ER 1590l	Koobi Fora (Kenya)	X				
Homo sp./*habilis s.l.*	KNM-ER 1590m	Koobi Fora (Kenya)		X			
Homo sp./*habilis s.l.*	SKX 268	Swartkrans (South Africa)	X				
Homo sp./*habilis s.l.*	KNM-ER 1813	Koobi Fora (Kenya)		X			
H. erectus s.l	KNM-ER 1808h	Koobi Fora (Kenya)		X			
H. erectus s.l	Sangiran 4	Sangiran, Java (Indonesia)	X	X			
H. erectus s.l	Sangiran 7-3b	Sangiran, Java (Indonesia)	X				
H. erectus s.l	Sangiran 7-3c	Sangiran, Java (Indonesia)		X			
Middle Pleistocene European hominins	Steinheim	Steinheim an der Murr (Germany)	X	X			
H. neanderthalensis	BD8	Abri Bourgeois-Delaunay, La Chaise Cave (France)	X	X			
H. neanderthalensis	Combe-Grenal IX	Combe-Grenal Cave (France)		X			
H. neanderthalensis	Combe-Grenal XIII	Combe-Grenal Cave (France)	X				
H. neanderthalensis	Kebara-dumps	Kebara Cave (Israel)					X
H. neanderthalensis	KMH 21	Kebara Cave (Israel)	X				
H. neanderthalensis	KMH 24	Kebara Cave (Israel)			X		
H. neanderthalensis	KRP 100	Krapina (Croatia)	X				
H. neanderthalensis	KRP 101	Krapina (Croatia)		X			
H. neanderthalensis	KRP 134	Krapina (Croatia)	X				
H. neanderthalensis	KRP 135	Krapina (Croatia)		X			
H. neanderthalensis	KRP 136	Krapina (Croatia)	X				
H. neanderthalensis	KRP 165	Krapina (Croatia)		X			
H. neanderthalensis	KRP 166	Krapina (Croatia)		X			
H. neanderthalensis	KRP 169	Krapina (Croatia)		X			
H. neanderthalensis	KRP 171	Krapina (Croatia)	X				
H. neanderthalensis	KRP 175	Krapina (Croatia)		X			

H. neanderthalensis	KRP 177	Krapina (Croatia)		X			
H. neanderthalensis	KRP 192	Krapina (Croatia)		X			
H. neanderthalensis	KRP 58	Krapina (Croatia)			X		
H. neanderthalensis	KRP 96	Krapina (Croatia)		X			
H. neanderthalensis	KRP 97	Krapina (Croatia)			X		
H. neanderthalensis	KRP 98	Krapina (Croatia)		X			
H. neanderthalensis	KRP 45	Krapina (Croatia)	X				
H. neanderthalensis	KRP 46	Krapina (Croatia)	X				
H. neanderthalensis	KRP 47	Krapina (Croatia)	X	X			
H. neanderthalensis	KRP 48	Krapina (Croatia)	X	X			
H. neanderthalensis	La Ferrassie 8	La Ferrasie (France)	X				
H. neanderthalensis	La Quina H18	La Quina (France)	X	X			
H. neanderthalensis	Le Moustier 1	Le Moustier (France)	X	X			
H. neanderthalensis	Roc de Marsal	Roc de Marsal (France)	X				
H. neanderthalensis	SCLA 4A-4	Scladina Cave (Belgium)	X				
H. neanderthalensis	SD 1105	El Sidrón (Spain)	X				
H. neanderthalensis	SD 407	El Sidrón (Spain)	X				
H. neanderthalensis	SD 531	El Sidrón (Spain)	X				
H. neanderthalensis	SD 4	El Sidrón (Spain)		X			
H. neanderthalensis	SD 551	El Sidrón (Spain)		X			
H. neanderthalensis	Saint-Césaire 1	La Roche a Pierrot, Saint-Césaire (France)		X			
H. sapiens (Pleistocene /early Holocene)	Combe-Capelle	Combe-Capelle (France)		X			
H. sapiens (Pleistocene)	Equus Cave H10	Equus Cave (South Africa)					X
H. sapiens (Pleistocene)	Oberkassel D999	Oberkassel (Germany)			X		
H. sapiens (Pleistocene)	Qafzeh 11	Qafzeh Cave (Israel)	X	X			
H. sapiens (Pleistocene)	Qafzeh 10	Qafzeh Cave (Israel)	X				
H. sapiens (Pleistocene)	Qafzeh 15	Qafzeh Cave (Israel)	X	X			
H. sapiens (Pleistocene)	Qafzeh9	Qafzeh Cave (Israel)		X			
H. sapiens (Pleistocene)	Skhūl I	Skhūl Cave (Israel)	X				

H. sapiens (Pleistocene)	Témara IB19	Contrebandiers, Témara (Morocco)	X	
H. sapiens (Pleistocene)	Témara T2	Contrebandiers, Témara (Morocco)		X

* The X indicates which tooth/teeth are represented for each specimen.

table S3. Fossil hominin lower molars used in this study including accession number, locality/site, and source.

Taxon	Specimen ID	Locality/Site (Country)	LM1	LM2	LM3	LM12	LM
A. anamensis	KNM-KP 34725r	Kanapoi (Kenya)	X				
A. anamensis	KNM-KP 29286	Kanapoi (Kenya)	X	X			
A. anamensis	KNM-KP 31712j	Kanapoi (Kenya)	X				
A. anamensis	KNM-ER 35233	Koobi Fora (Kenya)		X			
A. anamensis	KNM-KP 29281	Kanapoi (Kenya)		X			
A. anamensis	KNM-KP 34725t	Kanapoi (Kenya)		X			
A. afarensis	AL 145-35	Hadar (Ethiopia)	X				
A. afarensis	AL 333w-1a	Hadar (Ethiopia)	X				
A. afarensis	AL 128-23	Hadar (Ethiopia)		X			
A. afarensis	AL 241-14	Hadar (Ethiopia)		X			
A. afarensis	AL 333w-1a	Hadar (Ethiopia)		X			
A. afarensis	AL 145-35	Hadar (Ethiopia)		X			
A. afarensis	AL 333w-32	Hadar (Ethiopia)			X		
A. afarensis	AL 188-1	Hadar (Ethiopia)			X		
A. africanus	MLD 2	Makapansgat (South Africa)		X			
A. africanus	STS 18	Sterkfontein (South Africa)	X				
A. africanus	STS 24	Sterkfontein (South Africa)	X				
A. africanus	STS 52b	Sterkfontein (South Africa)	X	X			
A. africanus	STS 9	Sterkfontein (South Africa)	X				
A. africanus	STW 123b	Sterkfontein (South Africa)	X				
A. africanus	STW 3	Sterkfontein (South Africa)		X			
A. africanus	STW 560d	Sterkfontein (South Africa)		X			
A. africanus	STW 586	Sterkfontein (South Africa)			X		
A. africanus	STW 106	Sterkfontein (South Africa)	X				
A. africanus	STW 109	Sterkfontein (South Africa)		X			
A. africanus	STW 133	Sterkfontein (South Africa)			X		
A. africanus	STW 14	Sterkfontein (South Africa)		X	X		
A. africanus	STW 142 (STW 312)	Sterkfontein (South Africa)			X		

A. africanus	STW 145	Sterkfontein (South Africa)	X		
A. africanus	STW 213	Sterkfontein (South Africa)		X	
A. africanus	STW 234	Sterkfontein (South Africa)		X	
A. africanus	STW 235	Sterkfontein (South Africa)		X	
A. africanus	STW 246	Sterkfontein (South Africa)	X		
A. africanus	STW 278	Sterkfontein (South Africa)			X
A. africanus	STW 308	Sterkfontein (South Africa)		X	
A. africanus	STW 309A	Sterkfontein (South Africa)	X		
A. africanus	STW 327	Sterkfontein (South Africa)	X		
A. africanus	STW 327	Sterkfontein (South Africa)		X	X
A. africanus	STW 364	Sterkfontein (South Africa)	X		
A. africanus	STW 384	Sterkfontein (South Africa)			X
A. africanus	STW 404	Sterkfontein (South Africa)			X
A. africanus	STW 412A	Sterkfontein (South Africa)		X	
A. africanus	STW 412B	Sterkfontein (South Africa)		X	
A. africanus	STW 421A	Sterkfontein (South Africa)	X		
A. africanus	STW 421B	Sterkfontein (South Africa)	X		
A. africanus	STW 424	Sterkfontein (South Africa)		X	
A. africanus	STW 491	Sterkfontein (South Africa)		X	X
A. africanus	STW 498c	Sterkfontein (South Africa)		X	X
A. africanus	STW 520	Sterkfontein (South Africa)			X
A. africanus	STW 537 (STW 269)	Sterkfontein (South Africa)		X	
A. africanus	STW 537	Sterkfontein (South Africa)		X	
A. africanus	STW 537	Sterkfontein (South Africa)			X
A. africanus	STW 537	Sterkfontein (South Africa)			X
A. africanus	STW 555	Sterkfontein (South Africa)		X	
A. africanus	STW 560a	Sterkfontein (South Africa)			X
A. africanus	STW 560b	Sterkfontein (South Africa)			X
A. africanus	STW 560e	Sterkfontein (South Africa)		X	
A. africanus	Taung	Taung (South Africa)	X	X	
A. africanus	TM 1520	Sterkfontein (South Africa)			X

P. aethiopicus	L62-17	Omo (Ethiopia)		X		
P. aethiopicus	L157-35	Omo (Ethiopia)		X		
P. boisei	KNM-ER 60802	Koobi Fora (Kenya)				X
P. boisei	KNM-ER 25520	Koobi Fora (Kenya)		X		
P. boisei	KNM-ER 15930	Koobi Fora (Kenya)		X		
P. boisei	L427-7	Omo (Ethiopia)		X		
P. boisei	Omo F203	Omo (Ethiopia)		X		
P. boisei	Omo 47-1973_1500	Omo (Ethiopia)			X	
P. robustus	DNH 18	Drimolen (South Africa)			X	
P. robustus	DNH 21	Drimolen (South Africa)			X	
P. robustus	DNH 46	Drimolen (South Africa)	X			
P. robustus	DNH 51	Drimolen (South Africa)			X	
P. robustus	DNH 60B	Drimolen (South Africa)	X			
P. robustus	DNH 60C	Drimolen (South Africa)		X		
P. robustus	DNH 8	Drimolen (South Africa)	X	X	X	
P. robustus	GDA 2	Gondolin (South Africa)		X		
P. robustus	SK 1587a	Swartkrans (South Africa)		X		
P. robustus	SK 1	Swartkrans (South Africa)		X		
P. robustus	SK 104	Swartkrans (South Africa)	X			
P. robustus	SK 1587a	Swartkrans (South Africa)	X			
P. robustus	SK 1587b	Swartkrans (South Africa)		X		
P. robustus	SK 1588	Swartkrans (South Africa)	X			
P. robustus	SK 22	Swartkrans (South Africa)			X	
P. robustus	SK 23	Swartkrans (South Africa)	X	X	X	
P. robustus	SK 25	Swartkrans (South Africa)	X	X		
P. robustus	SK 34	Swartkrans (South Africa)		X		
P. robustus	SK 3974	Swartkrans (South Africa)	X			
P. robustus	SK 3978	Swartkrans (South Africa)	X			
P. robustus	SK 6	Swartkrans (South Africa)	X	X	X	
P. robustus	SK 61	Swartkrans (South Africa)	X			
P. robustus	SK 62	Swartkrans (South Africa)	X			

P. robustus	SK 63	Swartkrans (South Africa)	X		
P. robustus	SK 64	Swartkrans (South Africa)	X		
P. robustus	SK 75	Swartkrans (South Africa)			X
P. robustus	SK 828	Swartkrans (South Africa)	X		
P. robustus	SK 843	Swartkrans (South Africa)	X	X	X
P. robustus	SK 846a	Swartkrans (South Africa)	X		
P. robustus	SK 851	Swartkrans (South Africa)			X
P. robustus	SK W5	Swartkrans (South Africa)	X	X	
P. robustus	SK X4446	Swartkrans (South Africa)	X	X	
P. robustus	SK X5002	Swartkrans (South Africa)			X
P. robustus	SK X5014	Swartkrans (South Africa)			X
P. robustus	TM1600	Kromdraai (South Africa)		X	X
Homo sp./*habilis s.l.*	DNH 67	Drimolen (South Africa)	X		
Homo sp./*habilis s.l.*	KNM-ER 1802	Koobi Fora (Kenya)	X	X	
Homo sp./*habilis s.l.*	KNM-ER 2597	Koobi Fora (Kenya)		X	
Homo sp./*habilis s.l.*	L26-1g	Omo (Ethiopia)	X		
Homo sp./*habilis s.l.*	Omo K7_1969_17	Omo (Ethiopia)	X		
Homo sp./*habilis s.l.*	SK 15	Swartkrans (South Africa)		X	X
Homo sp./*habilis s.l.*	SKX 258	Swartkrans (South Africa)	X		
H. erectus s.l.	S1b	Sangiran, Java (Indonesia)	X	X	
H. erectus s.l.	KNM-BK 67	Baringo Kapthurin (Kenya)		X	X
Middle Pleistocene European hominins	Mauer	Mauer (Germany)	X	X	X
H. neanderthalensis	La Chaise 14-7	Abri Bourgeois-Delaunay, La Chaise Cave (France)	X		
H. neanderthalensis	La Chaise 49	Abri Bourgeois-Delaunay, La Chaise Cave (France)	X		
H. neanderthalensis	La Chaise 5	Abri Bourgeois-Delaunay, La Chaise Cave (France)	X		
H. neanderthalensis	Combe-Grenal I	Combe-Grenal Cave (France)	X		
H. neanderthalensis	Combe-Grenal IV	Combe-Grenal Cave (France)	X		

H. neanderthalensis	1048/69	Weimar - Ehringsdorf (Germany)	X		
H. neanderthalensis	KRP 9	Krapina (Croatia)			X
H. neanderthalensis	La Chaise 36	Abri Bourgeois-Delaunay, La Chaise Cave (France)			X
H. neanderthalensis	KMH 14	Kebara Cave (Israel)		X	
H. neanderthalensis	KMH 18	Kebara Cave (Israel)		X	
H. neanderthalensis	KMH 4	Kebara Cave (Israel)	X		
H. neanderthalensis	KRP 57	Krapina (Croatia)		X	
H. neanderthalensis	KRP 59	Krapina (Croatia)		X	
H. neanderthalensis	KRP 52	Krapina (Croatia)	X		
H. neanderthalensis	KRP 1	Krapina (Croatia)		X	
H. neanderthalensis	KRP 106	Krapina (Croatia)			X
H. neanderthalensis	KRP 107	Krapina (Croatia)		X	
H. neanderthalensis	KRP 6	Krapina (Croatia)		X	
H. neanderthalensis	KRP 10	Krapina (Croatia)		X	
H. neanderthalensis	KRP 104	Krapina (Croatia)		X	
H. neanderthalensis	KRP 105	Krapina (Croatia)		X	
H. neanderthalensis	KRP 53	Krapina (Croatia)	X	X	
H. neanderthalensis	KRP 54	Krapina (Croatia)	X	X	
H. neanderthalensis	KRP 55	Krapina (Croatia)	X	X	
H. neanderthalensis	KRP 79	Krapina (Croatia)	X		
H. neanderthalensis	KRP 80	Krapina (Croatia)		X	
H. neanderthalensis	KRP 81	Krapina (Croatia)	X		
H. neanderthalensis	KRP 86	Krapina (Croatia)		X	
H. neanderthalensis	La Quina H9	La Quina (France)		X	
H. neanderthalensis	La Chaise 36	Abri Bourgeois-Delaunay, La Chaise Cave (France)		X	
H. neanderthalensis	LaFerrassie_8	La Ferrasie (France)	X		
H. neanderthalensis	Le Moustier 1 (left side)	Le Moustier (France)		X	X

H. neanderthalensis	Le Moustier 1 (right side)	Le Moustier (France)		X			
H. neanderthalensis	Regourdou	Le Regourdou, Montignac (France)		X	X		
H. neanderthalensis	Roc de Marsal	Roc de Marsal (France)	X				
H. neanderthalensis	Scla 4A-1	Scladina Cave (Belgium)	X	X	X		
H. neanderthalensis	SD 540	El Sidrón (Spain)		X			
H. neanderthalensis	SD 780	El Sidrón (Spain)	X				
H. neanderthalensis	SD 755	El Sidrón (Spain)		X			
H. neanderthalensis	SR 756	El Sidrón (Spain)	X				
H. neanderthalensis	Vi 11-39	Vindija (Croatia)		X	X		
H. sapiens (Pleistocene)	DES H4	Dar es Soltane II (Morocco)		X	X		
H. sapiens (Pleistocene)	El Harhoura	El Harhoura (Morocco)		X	X		
H. sapiens (Pleistocene)	Equus Cave H3	Equus Cave (South Africa)			X		
H. sapiens (Pleistocene)	Equus Cave H5	Equus Cave (South Africa)					X
H. sapiens (Pleistocene)	Equus Cave H8	Equus Cave (South Africa)		X			
H. sapiens (Pleistocene)	Hayonim 17	Hayonim (Israel)		X			
H. sapiens (Pleistocene)	Hayonim 19	Hayonim (Israel)		X	X		
H. sapiens (Pleistocene)	Hayonim 20	Hayonim (Israel)			X		
H. sapiens (Pleistocene)	Hayonim 8	Hayonim (Israel)			X		
H. sapiens (Pleistocene)	Irhoud 3	Jebel Irhoud (Morocco)	X				
H. sapiens (Pleistocene)	Nahal-Oren 8	Nahal Oren (Israel)		X	X		
H. sapiens (Pleistocene)	Qafzeh 10	Qafzeh Cave (Israel)		X			
H. sapiens (Pleistocene)	Qafzeh 11	Qafzeh Cave (Israel)		X	X		
H. sapiens (Pleistocene)	Qafzeh 15	Qafzeh Cave (Israel)	X	X			
H. sapiens (Pleistocene)	SAM AP 6242	Die Kelders (South Africa)					X
H. sapiens (Pleistocene)	SAM AP 6277	Die Kelders (South Africa)					X
H. sapiens (Pleistocene)	Témara	Contrebandiers, Témara (Morocco)		X	X		
H. sapiens (Pleistocene)	Témara T3a	Contrebandiers, Témara (Morocco)	X				

* The X indicates which tooth/teeth are represented for each specimen.

table S4. System used in this study for scoring accessory cusps.

Trait expression	
ASUDAS* for UMC5, LMC5, LMC6 and LMC7	**Simplified scoring**
0: cusp is absent	Absent
0.5: indecisive category	Suspected
1: cusp is present and very small	Faint
2: cusp is small 3: cusp is medium-sized	Moderate
4: cusp is large 5: cusp is very large	Large
Scoring system for hypocone, UMC6 and LMC6 "double"	**Simplified scoring**
0/1: Hypocone	Absent/Present
0/1: UMC6	Absent/Present
0/1: LMC6 "double"	Absent/Present
ASUDAS for Carabelli's cusp in *Homo*	**Simplified scoring**
0: the mesiolingual aspect of cusp 1 is smooth	Absent
1: a groove is present 2: a pit is present	Faint
3: a small [or medium-sized] Y-shaped depression is present 4: a large Y-shaped depression is present	Moderate
5: a small cusp without a free apex occurs. The distal border of the cusp does not contact the lingual groove separating cusps 1 and 4 6: a medium-sized cusp with an attached apex making contact with the medial lingual groove is present 7: a large cusp is present	Large
Scoring system from van Reenen and Reid (*40*) for Carabelli's cusp in *Australopithecus* and *Paranthropus*	**Simplified scoring**
0: the mesiolingual aspect of cusp 1 is smooth	Absent
1: the lingual cingulum is reduced to one or two short furrows or a single pit which may be fairly deep. The wrinkles are usually less prominent in this category but may have contributed to the formation of the short furrows which may be horizontal, vertical or oblique in direction	Faint
2: the lingual cingulum decreases further in length and prominence and together with the vertical furrows of wrinkled enamel produces a feature of great variability. There are usually between 3-7 vertical furrows on the protocone which sometimes branch at the occlusal end 3: the cingulum decreases further in length and prominence but the cuspules are larger	Moderate
4: the cingulum is usually shorter in length but carries one or more cuspules which may break the continuity of the furrow 5: a complete lingual cingulum is present extending from the mesio-buccal corner of the crown traversing the lingual surface of the protocone in an oblique cervical direction and terminating in the occluso-lingual groove. Wrinkles on the enamel surface cross the cingulum in a vertical direction at almost right angles and on the cervical border of the cingulum usually produce small rounded bulges between each wrinkle	Large
Scoring system from Ortiz et al. (*25*) for Carabelli's cusp in great apes	**Simplified scoring**
0: the mesiolingual aspect of the protocone is smooth	Absent
1: one or many minor depressions or vertical furrows are present on the mesiolingual aspect of the protocone	Faint
2: a crest is present but is limited to the mesiolingual aspect of the protocone 3: a continuous, or semi-continuous, crest extends distally and traverses the lingual aspect of the protocone of the protocone. Although the crest is confined to the protocone, it may contact the median lingual groove separating the protocone and hypocone	Moderate
4: a continuous, or semi-continuous, crest traverses the lingual aspect of the protocone and extends distally onto the hypocone	Large

*ASUDAS (ref. *36*) with some minor modifications.

table S5. Tooth size comparisons estimated from crown outline, centroid size, and 3D surface area. For each UM and LM, yellow triangle: correlation coefficient with significant values bolded; gray triangle: slope / intercept of ordinary least square linear regression. Comparisons performed on the logged data.

UM	Crown outline	Centroid size	3D surface area
Crown outline	-	1.072/-0.388	1.222/-0.625
Centroid size	**0.878**	-	1.140/-0.221
3D surface area	**0.856**	**0.881**	-

LM	Crown outline	Centroid size	3D surface area
Crown outline	-	1.112/-0.488	1.146/-0.474
Centroid size	**0.905**	-	1.030/0.012
3D surface area	**0.906**	**0.912**	-